Title	Dynamic photoelectrothermal theory for light-emitting diode systems
Author(s)	Tao, X; Hui, SYR
Citation	IEEE Transactions on Industrial Electronics, 2012, v. 59 n. 4, p. 1751-1759
Issued Date	2012
URL	http://hdl.handle.net/10722/155689
Rights	IEEE Transactions on Industrial Electronics. Copyright © IEEE

Dynamic Photoelectrothermal Theory for Light-Emitting Diode Systems

Xuehui Tao and S. Y. Ron Hui, *Fellow, IEEE*

***Abstract*—This paper presents a dynamic photoelectrothermal theory for light-emitting diode (LED) systems. In addition to photometric, electrical, and thermal aspects, this theory incorporates the time domain into the generalized equations. A dynamic model for a general LED system is developed for system analysis. This theory highlights the fact that the luminous output of an LED system will decrease with time from the initial operation to the steady state due to the rising temperature of the heat sink and the LED devices. The essential thermal time constants involved in the LED systems are explained. The time factor is critical in understanding how much the luminous output will decrease with time and is essential to the optimal designs of the LED systems that are operated continuously (e.g., general lighting) or momentarily (e.g., traffic lights). Experiments on several LED systems at different time frames have been conducted, and the practical measurements confirm the validity of this theory.**

***Index Terms*—Light-emitting diodes (LEDs), lighting systems.**

I. Introduction

In A RECENT Institution of Engineering and Technology article on lighting [1], comments are quoted about light-emitting diode (LED) products that "the majority of LED A-type replacement lamps do not meet manufacturer performance claims" and that "testing reveals that these lamps produce only 10% to 60% of their claimed light output." Aside from the quality issues, one possible reason for such mismatch in the claimed and actual luminous performance is the misunderstanding of the luminous efficacy figures of the LED devices. LED device manufacturers usually cite high luminous efficacy figures which are only correct at a junction temperature of 25 °C. In practice, luminous efficacy will decrease significantly with increasing LED junction temperature [2]–[5]. At a junction temperature under normal operation, it is not unusual that the luminous efficacy could drop by 25% or more [6].

Unlike traditional power electronic circuits, the main factor that needs to be optimized in a lighting system is the luminous efficacy [7], [20] instead of the energy efficiency [18]. Good luminous efficacy would automatically imply good efficiency, but not vice versa. The general (steady-state) photoelectrothermal (PET) theory for LED systems [7] has pointed out both theoretically and practically that an LED device will not necessarily generate the maximum amount of luminous output at its rated power unless the LED system is optimally designed in an integrated manner. Optimal design of LED systems can only be achieved with the proper choices of LED devices and array structure, LED driver, operating power, and thermal design. Various aspects of LED systems, such as the thermal management [8]–[11], nonlinear behavior of junction-to-case thermal resistance [12], LED drivers [13], [18], and current-sharing techniques for LED strings [14], [15], have been reported. While the interactions of photometric, electric, and thermal aspects of the LED systems have been linked together [7], [16], very limited research on the time dependence of the luminous performance of LED systems has been reported.

This time factor is in fact highly relevant to the actual luminous output of any LED system. For LED systems designed for continuous operation, such as road lighting systems and LED bulbs, the luminous output will drop from the initial operation to the steady state. The main reason is due to the gradual increase in the LED junction and heat-sink temperature values. Therefore, the time factor is critical in understanding how much luminous reduction an LED system will have so that proper LED systems can be designed. For LED systems with momentary or discontinuous operation, such as traffic lights and signal indicators of vehicles, the design criteria would be different from those for continuous operation. The PET theory [7] published in 2009 describes the steady-state performance of an LED system. As an extended version of [19], this paper incorporates the time domain into the PET theory so that the dynamic behavior of the LED systems can be studied in the time domain. This dynamic PET theory will converge to the steady-state theory under steady-state conditions. Since the luminous efficacy is the main design factor for LED systems, this dynamic theory provides a useful tool not only for studying the behavior of LED systems but also, more importantly, for optimizing LED system designs for both continuous and discontinuous operations.

II. Dynamic PET Theory for LED Systems

A. Dynamic Equivalent Circuit for an LED System

Fig. 1 shows the thermal equivalent circuit of one LED mounted on a heat sink. The heat source P_{heat} is the amount of heat generated by the LED. The internal junction temperature of the LED device is T_j. The thermal resistor and thermal

Manuscript received August 18, 2010; revised October 19, 2010 and December 8, 2010; accepted December 16, 2010. Date of publication January 28, 2011; date of current version November 1, 2011. This work was supported by the Centre for Power Electronics, City University of Hong Kong.

X. Tao is with the Centre for Power Electronics, Department of Electronic Engineering, City University of Hong Kong, Kowloon, Hong Kong (e-mail: eeronhui@cityu.edu.hk).

S. Y. R. Hui is with the Department of Electrical and Electronic Engineering, The University of Hong Kong, Hong Kong, and also with the Department of Electrical and Electronic Engineering, Imperial College London, SW7 2AZ London, U.K. (e-mail: ronhui@eee.hku.hk; r.hui@imperial.ac.uk).

Color versions of one or more of the figures in this paper are available online at http://ieeexplore.ieee.org.

Digital Object Identifier 10.1109/TIE.2011.2109341

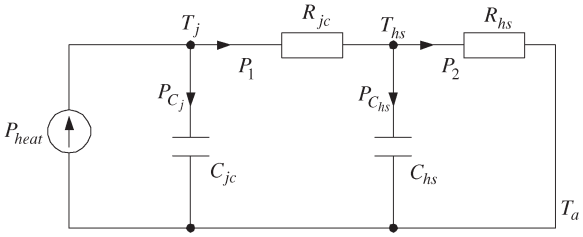

Fig. 1. Dynamic thermal equivalent circuit of one LED mounted on a heat sink.

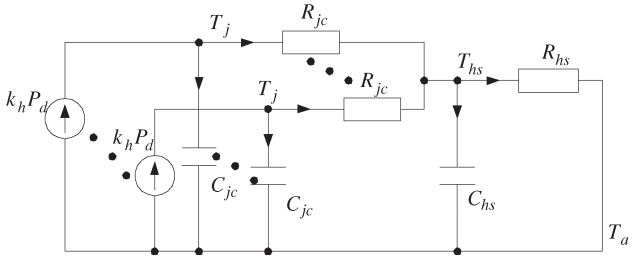

Fig. 2. Dynamic thermal equivalent circuit of N LEDs mounted on the same heat sink.

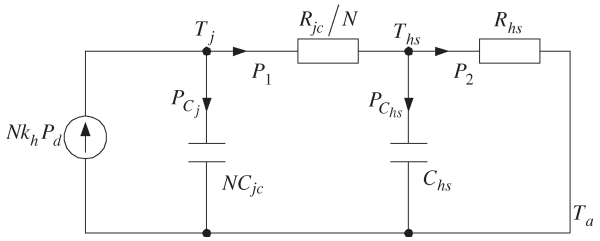

Fig. 3. Simplified dynamic thermal equivalent circuit of N LEDs mounted on the same heat sink.

capacitor of the LED device are labeled as R_{jc} and C_{jc}, respectively. T_{hs} is the heat-sink surface temperature, and R_{hs} and C_{hs} are the heat sink's thermal resistor and thermal capacitor, respectively. In practice, the LED package is mounted on the heat sink with some form of electrical insulation or with the use of thermal paste to ensure good thermal contact. The thermal resistance of this thermally conductive layer is usually much smaller than R_{jc} and R_{hs} and is thus ignored in the following analysis.

If a number of N LED devices are assumed to be mounted on the same heat sink, the dynamic thermal equivalent circuit is shown in Fig. 2. Assuming that the temperature is distributed uniformly and the junction temperature of the LEDs is identical, the dynamic thermal equivalent circuit of Fig. 2 can be simplified as shown in Fig. 3.

B. Dynamic PET Theory

The amount of heat generated by an LED can be expressed as

$$P_{\text{heat}} = k_h P_d \tag{1}$$

where k_h is the heat dissipation coefficient that represents the portion of input power that is dissipated as heat [17] and P_d is the input power of each LED.

In Fig. 3, some heat (P_1) flows from the equivalent heat source through the equivalent thermal resistor, and another portion of the heat (P_{Cj}) flows into the equivalent thermal capacitor of the LED package. Based on the thermal circuit analysis, it can be shown that

$$P_{C_j} = Nk_hP_d - P_1 \tag{2}$$

$$P_{C_j} = NC_{jc}\frac{d(T_j - T_a)}{dt} \tag{3}$$

$$P_1 = \frac{T_j - T_{hs}}{R_{jc}/N}. \tag{4}$$

Based on (2)–(4)

$$NC_{jc}\frac{d(T_j - T_a)}{dt} = Nk_hP_d - \frac{T_j - T_{hs}}{R_{jc}/N}. \tag{5}$$

Rearranging (5) gives

$$\frac{dT_j}{dt} + \frac{1}{C_{jc}R_{jc}}T_j = \frac{k_hP_d}{C_{jc}} + \frac{T_{hs}}{C_{jc}R_{jc}}. \tag{6}$$

In practice, the thermal time constant of the LED package $(\tau_{jc} = R_{jc}C_{jc})$ is much smaller than that of the heat sink $(\tau_{hs} = R_{hs}C_{hs})$. The heat-sink temperature T_{hs} will change much slowly than the LED junction temperature T_j. In order to avoid confusion, the terms "fast transient" and "slow transient" refer to the time frames in the order of the τ_{jc} and τ_{hs}, respectively. Under a fast-transient situation, T_{hs} can be considered as a constant. Based on this argument, the dynamic relationship between T_j and T_{hs} under fast-transient condition can be obtained from (6) as

$$T_j = R_{jc}k_hP_d\left(1 - e^{-\frac{t}{C_{jc}R_{jc}}}\right) + T_{hs}. \tag{7}$$

For the heat sink, the heat flows into the thermal capacitor C_{hs} and the thermal resistor R_{hs} of the heat sink. The heat flow component P_1 can be expressed as

$$P_1 = P_{C_{hs}} + P_2 \tag{8}$$

where P_{Chs} is the heat flowing into the thermal capacitor of the heat sink and P_2 is the heat through the thermal resistor of the heat sink. They can be formulated as

$$P_{C_{hs}} = C_{hs}\frac{d(T_{hs} - T_a)}{dt} \tag{9}$$

$$P_2 = \frac{T_{hs} - T_a}{R_{hs}}. \tag{10}$$

From (4) and (8)–(10), the heat-sink temperature is therefore

$$\frac{T_j - T_{hs}}{R_{jc}/N} = C_{hs}\frac{d(T_{hs} - T_a)}{dt} + \frac{T_{hs} - T_a}{R_{hs}} \tag{11}$$

which can be rewritten as

$$\frac{dT_{hs}}{dt} = \frac{N}{C_{hs}R_{jc}}T_j - \frac{NR_{hs} + R_{jc}}{C_{hs}R_{hs}R_{jc}}T_{hs} + \frac{T_a}{C_{hs}R_{hs}}. \tag{12}$$

Now, the relationship of T_j and T_{hs} obtained in (7) can be used in (12)

$$\frac{dT_{hs}}{dt} = \left[\frac{N}{C_{hs}R_{jc}}\left(-R_{jc}k_hP_de^{-\frac{t}{C_{jc}R_{jc}}} + R_{jc}k_hP_d + T_{hs}\right) - \frac{NR_{hs}+R_{jc}}{C_{hs}R_{hs}R_{jc}}T_{hs} + \frac{T_a}{C_{hs}R_{hs}}\right]. \quad (13)$$

Solving (13), the heat-sink temperature T_{hs} can be obtained as

$$T_{hs}(t) = \left[\frac{-R_{jc}C_{jc}NR_{hs}k_hP_d}{C_{jc}R_{jc}-C_{hs}R_{hs}}e^{-\frac{t}{C_{jc}R_{jc}}} + NR_{hs}k_hP_d + Ae^{-\frac{t}{C_{hs}R_{hs}}} + T_a\right] \quad (14)$$

where A represents a constant, which can be determined from the physical boundary condition of the heat sink. The boundary condition of a heat sink is that, at $t = 0$, the heat-sink temperature is equal to the ambient temperature. That is

$$T_{hs}(t=0) = T_a. \quad (15)$$

Putting (15) into (14), the coefficient A can be obtained as

$$A = -\left(\frac{-R_{jc}C_{jc}NR_{hs}k_hP_d}{C_{jc}R_{jc}-C_{hs}R_{hs}} + NR_{hs}k_hP_d\right).$$

Putting A into (14), the heat-sink temperature can be obtained as

$$T_{hs}(t) = \left[\frac{-R_{jc}C_{jc}Nk_hP_dR_{hs}}{C_{jc}R_{jc}-C_{hs}R_{hs}}e^{-\frac{t}{C_{jc}R_{jc}}} + \frac{Nk_hP_dR_{hs}^2C_{hs}}{C_{jc}R_{jc}-C_{hs}R_{hs}}e^{-\frac{t}{C_{hs}R_{hs}}} + NR_{hs}k_hP_d + T_a\right]. \quad (16)$$

By putting the result of (16) into (7), the complete dynamic LED junction temperature T_j is

$$T_j = \left[-R_{jc}k_hP_d\left(\frac{C_{jc}NR_{hs}}{C_{jc}R_{jc}-C_{hs}R_{hs}}+1\right)e^{-\frac{t}{C_{jc}R_{jc}}} + k_hP_d\frac{NR_{hs}^2C_{hs}}{C_{jc}R_{jc}-C_{hs}R_{hs}}e^{-\frac{t}{C_{hs}R_{hs}}} + (R_{jc}+NR_{hs})k_hP_d + T_a\right]. \quad (17)$$

The luminous efficacy (E) has the following relationship with the junction temperature T_j of the LED [7]:

$$E = E_o\left[1 + k_e(T_j - T_o)\right]. \quad (18)$$

Now, T_j obtained in (17) can be used in (18)

$$E = E_o\left[1 + k_e(T_a - T_o) + k_ek_h(R_{jc}+NR_{hs})P_d - k_eR_{jc}k_hP_d\left(\frac{NR_{hs}C_{jc}}{C_{jc}R_{jc}-C_{hs}R_{hs}}+1\right)e^{-\frac{t}{C_{jc}R_{jc}}} + k_ek_hP_d\frac{NR_{hs}^2C_{hs}}{C_{jc}R_{jc}-C_{hs}R_{hs}}e^{-\frac{t}{C_{hs}R_{hs}}}\right]. \quad (19)$$

Therefore, the total luminous flux ϕ_v is

$$\phi_v = NEP_d$$

$$\phi_v = NE_o\left\{\left[1 + k_e(T_a - T_o)\right]P_d + k_ek_h(R_{jc}+NR_{hs})P_d^2 - k_ek_hR_{jc}\left(\frac{NR_{hs}C_{jc}}{C_{jc}R_{jc}-C_{hs}R_{hs}}+1\right)\times e^{-\frac{t}{C_{jc}R_{jc}}}P_d^2 + k_ek_h\frac{NR_{hs}^2C_{hs}}{C_{jc}R_{jc}-C_{hs}R_{hs}}\times e^{-\frac{t}{C_{hs}R_{hs}}}P_d^2\right\}. \quad (20)$$

Equations (16)–(20) now form the set of dynamic equations that describe the essential variables of the LED system. These dynamic equations can converge to the steady-state equations as the time variable t approaches infinity.

As $t \to \infty$, (16) becomes

$$T_{hs}(t) = NR_{hs}k_hP_d + T_a \quad (21)$$

(17) becomes

$$T_j = (R_{jc}+NR_{hs})k_hP_d + T_a \quad (22)$$

(19) becomes

$$E = E_o\left[1 + k_e(T_a - T_o) + k_ek_h(R_{jc}+NR_{hs})P_d\right] \quad (23)$$

and (20) becomes

$$\phi_v = NE_o\left\{\left[1 + k_e(T_a - T_o)\right]P_d + k_ek_h(R_{jc}+NR_{hs})P_d^2\right\}. \quad (24)$$

It can be seen that (21)–(24) are identical to the steady-state equations of the general PET theory reported in [7]. In practice, the ventilation of a LED system is affected by the lighting fixture design. In this case, the heat-sink thermal resistance should be measured in the presence of the lighting fixture. By warming up the heat sink with a known resistor driven by a given power, the thermal time constant of the heat sink can be extracted [19].

III. Experimental Verification

Three types of LED devices are used to evaluate the validity of the dynamic PET theory. Each type of LED device is mounted on two different heat sinks, and the luminous outputs and LED power levels are recorded at several intervals during the test periods. Luminous and power measurements are taken with the use of a spectrophotocolorimeter system that includes accessories such as integrating sphere and power supplies. The current of the LEDs is controlled by an adjustable power supply with constant current control. The heat sinks on which the LEDs are mounted are placed on one side of the internal surface of an integrating sphere for luminous measurements. Thermal couplers are mounted on the heat sinks in order to monitor the temperature rise of the heat sinks, and the temperature values are recorded with a data logger. Although it is not advisable to operate the LEDs beyond their rated power, the LEDs in

TABLE I
LED SYSTEM PARAMETERS

k_e	k_h	E_o	T_a	T_o	N	R_{hs}	R_{jc}	τ_{LED}	τ_{hs}
-0.0053	0.9	36	28	25	4	10	15	0.3	450

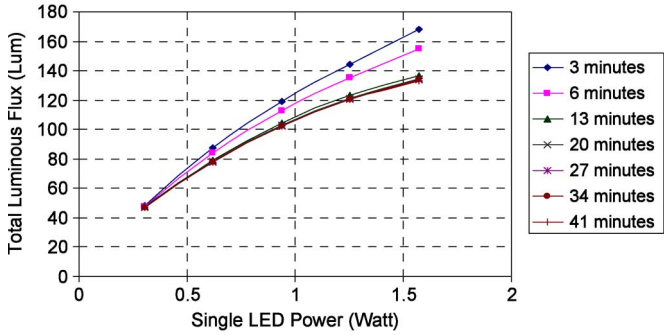

Fig. 4. Measured luminous flux for four Philips-Luxeon LEDs mounted on a heat sink with $R_{hs} = 10$ °C/W.

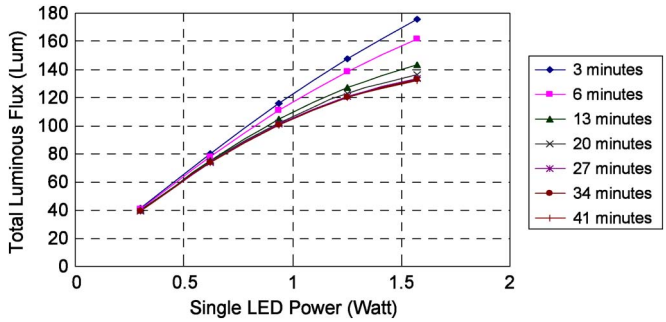

Fig. 5. Calculated luminous flux for four Philips-Luxeon LEDs mounted on a heat sink with $R_{hs} = 10$ °C/W.

these tests are powered beyond their rated values in order to provide more data for verifying the dynamic PET theory. The thermal time constants of the LED devices are obtained from the measurements using the T3ster system. Those of the heat sinks are estimated from the temperature reduction curves of the heat sinks (obtained by heating the heat sink to a certain temperature and then letting it cool down naturally). Other parameters are obtained from the manufacturers' data sheets or from previous measurements.

A. Tests on Philips-Luxeon 1-W LEDs (Model Number: LXHL-PW01)

In each test, four Luxeon 1-W LEDs are mounted on the heat sink, and the luminous flux curves are recorded at different time intervals. The thermal resistances of the heat sink Sample A and Sample B are 10 °C/W and 7.1 °C/W, respectively. Table I shows the measured data.

1) On a Heat Sink With Thermal Resistance of 10 °C/W: The curves of the luminous flux are measured and recorded at different time intervals as shown in Fig. 4. The parameters $\tau_{\rm LED}$, τ_{hs}, and R_{hs} have already been measured and are listed in Table I. Based on the dynamic PET theory, the theoretical curves of the luminous flux obtained from (20) at the same time intervals are plotted in Fig. 5. These results are in agreement in general.

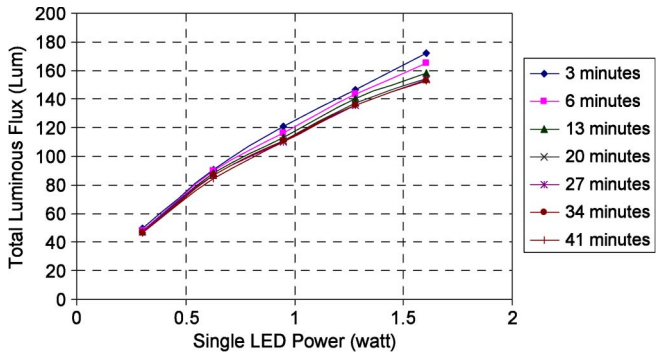

Fig. 6. Measured luminous flux for four Philips-Luxeon LEDs mounted on a heat sink with $R_{hs} = 7.1$ °C/W.

TABLE II
LED SYSTEM PARAMETERS

k_e	k_h	E_o	T_a	T_o	N	R_{hs}	R_{jc}	τ_{LED}	τ_{hs}
-0.0053	0.9	36	28	25	4	7.1	15	0.3	500

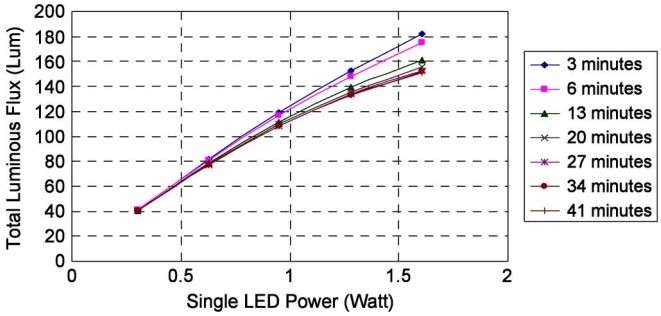

Fig. 7. Calculated luminous flux for four Philips-Luxeon LEDs mounted on a heat sink with $R_{hs} = 7.1$ °C/W.

TABLE III
LED SYSTEM PARAMETERS

k_e	k_h	E_o	T_a	T_o	N	R_{hs}	R_{jc}	τ_{LED}	τ_{hs}
-0.005	0.87	100	28	25	8	2.9	8	0.45	510

2) On a Heat Sink With Thermal Resistance of 7.1 °C/W: The measured luminous flux curves at different time intervals are shown in Fig. 6. Using the parameters shown in Table II, the theoretical curves are obtained and plotted in Fig. 7. The measured and theoretical results show good agreement.

B. Tests on CREE XLamp XR-E 3-W LEDs (Model Number: XREWHT-L1-WG-Q5-0-04)

Eight CREE 3-W LEDs are mounted on heat sinks in two sets of tests with the heat-sink thermal resistance equal to 2.9 °C/W (Sample C) and 1.8 °C/W (Sample D). Table III shows the measured data.

1) On a Heat Sink With Thermal Resistance of 2.9 °C/W: The measured luminous flux curves are shown in Fig. 8. For the theoretical curves, the parameters $\tau_{\rm LED}$, τ_{hs}, and R_{hs} are listed in Table III. The theoretical luminous flux curves versus the LED power at different time intervals generated by (20) are

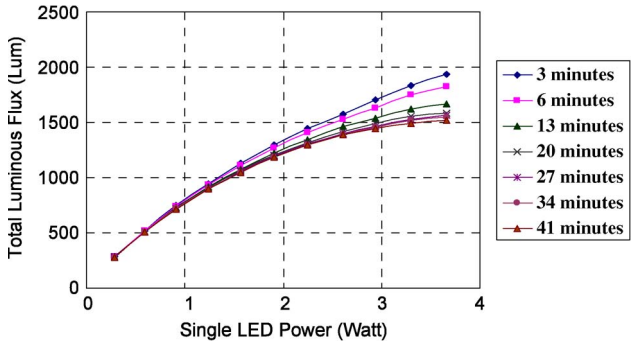

Fig. 8. Measured luminous flux for eight CREE XLamp XR-E LEDs mounted on a heat sink with $R_{hs} = 2.9$ °C/W.

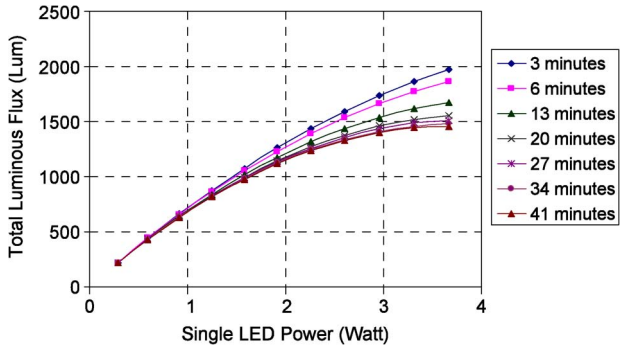

Fig. 9. Calculated luminous flux for eight CREE XLamp XR-E LEDs mounted on a heat sink with $R_{hs} = 2.9$ °C/W.

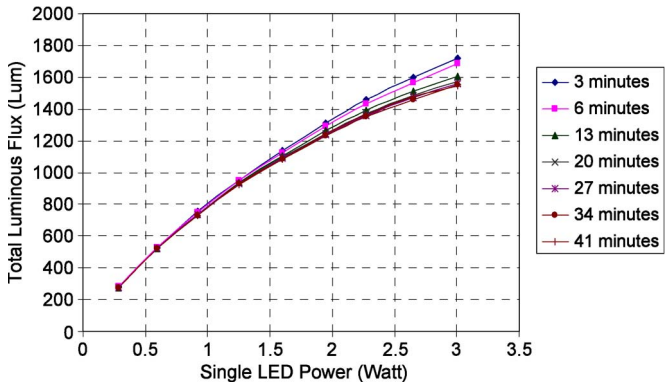

Fig. 10. Measured luminous flux for eight CREE XLamp XR-E LEDs mounted on a heat sink with $R_{hs} = 1.8$ °C/W.

TABLE IV
LED SYSTEM PARAMETERS

k_e	k_h	E_o	T_a	T_o	N	R_{hs}	R_{jc}	τ_{LED}	τ_{hs}
-0.0058	0.87	100	28	25	8	1.8	8	0.45	520

plotted in Fig. 9. Very good agreements between the measured and theoretical curves are observed.

2) On a Heat Sink With Thermal Resistance of 1.8 °C/W: The curves of the luminous flux are measured and recorded at different time intervals as shown in Fig. 10. The parameters $\tau_{\rm LED}$, τ_{hs}, and R_{hs} have already been measured and are listed in Table IV. Based on the dynamic PET theory, the theoretical curves of the luminous flux obtained from (20) at the same time intervals are plotted in Fig. 11.

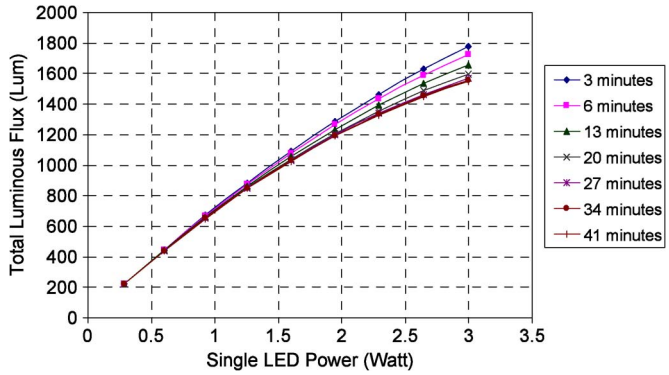

Fig. 11. Calculated luminous flux for eight CREE XLamp XR-E LEDs mounted on a heat sink with $R_{hs} = 1.8$ °C/W.

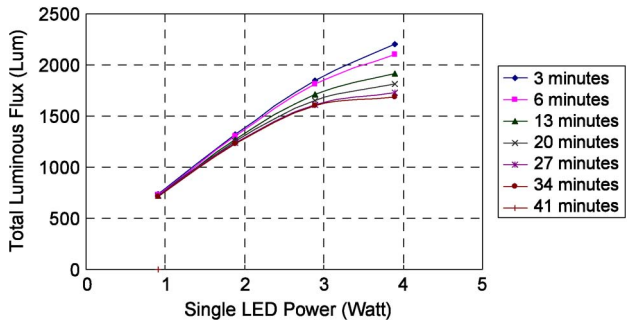

Fig. 12. Measured luminous flux for eight SHARP 3-W LEDs mounted on a heat sink with $R_{hs} = 2.9$ °C/W.

TABLE V
LED SYSTEM PARAMETERS

k_e	k_h	E_o	T_a	T_o	N	R_{hs}	R_{jc}	τ_{LED}	τ_{hs}
-0.0045	0.87	104	28	25	8	2.9	6.5	0.75	510

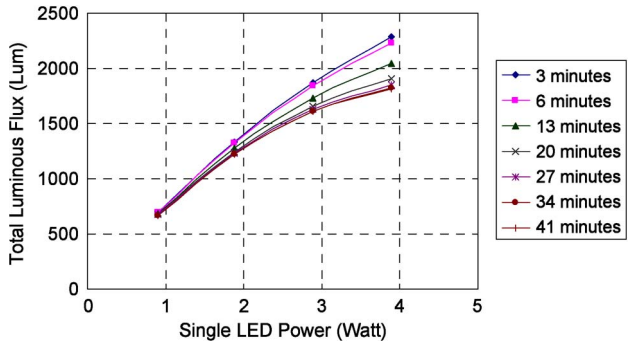

Fig. 13. Calculated luminous flux for eight SHARP 3-W LEDs mounted on a heat sink with $R_{hs} = 2.9$ °C/W.

C. Tests on SHARP 3-W LEDs

Similar tests are repeated on eight SHARP 3-W LEDs mounted on heat sinks—Sample C and Sample D.

1) On a Heat Sink With Thermal Resistance of 2.9 °C/W: The measured luminous flux curves at different time intervals are shown in Fig. 12. Table V shows the parameters used for the theoretical prediction, and the theoretical curves are shown in Fig. 13.

2) On a Heat Sink With Thermal Resistance of 1.8 °C/W: The measured luminous flux at different time intervals is

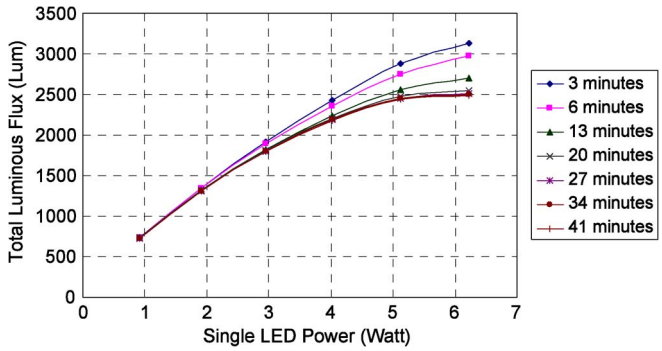

Fig. 14. Measured luminous flux for eight SHARP 3-W LEDs mounted on a heat sink with $R_{hs} = 1.8$ °C/W.

TABLE VI
LED SYSTEM PARAMETERS

k_e	k_h	E_o	T_a	T_o	N	R_{hs}	R_{jc}	τ_{LED}	τ_{hs}
-0.0045	0.87	104	28	25	8	1.8	6.5	0.75	520

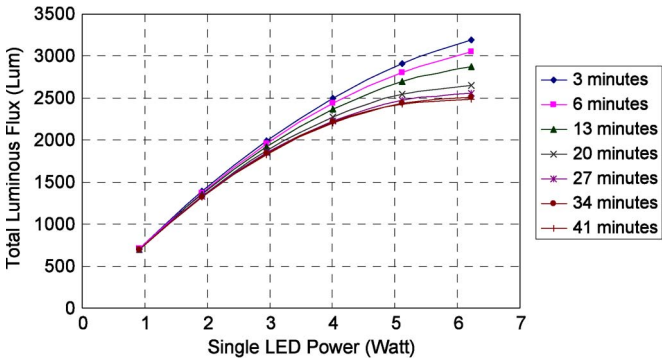

Fig. 15. Calculated luminous flux for eight SHARP 3-W LEDs mounted on a heat sink with $R_{hs} = 1.8$ °C/W.

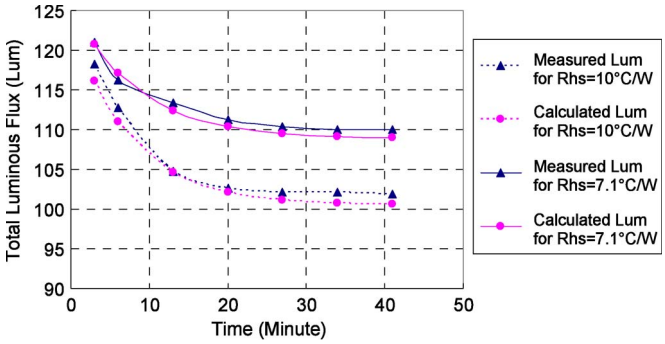

Fig. 16. Variation of the luminous flux with time for four Luxeon 1-W LEDs operated at rated power.

recorded in Fig. 14. With the parameters listed in Table VI, the theoretical luminous flux curves are plotted in Fig. 15. These results agree well with the measurements.

IV. REDUCTION OF LUMINOUS FLUX WITH TIME

Based on the practical and theoretical results obtained in Section III, the variations of the luminous flux with time under the operations at rated power for the three types of LEDs are shown in Fig. 16 (Luxeon 1-W LEDs), Fig. 17 (CREE 3-W LEDs), and Fig. 18 (SHARP 3-W LEDs). When mounted on

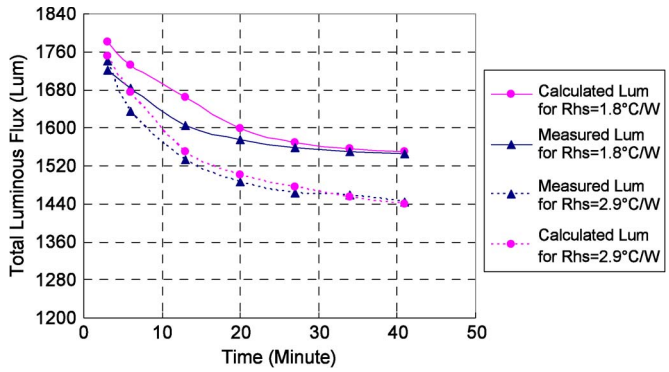

Fig. 17. Variation of the luminous flux with time for eight CREE 3-W LEDs operated at rated power.

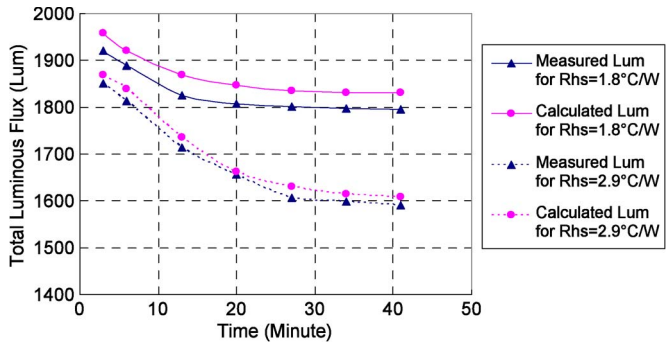

Fig. 18. Variation of the luminous flux with time for eight SHARP 3-W LEDs operated at rated power.

a heat sink with $R_{hs} = 2.9$ °C/W, both CREE 3-W LEDs and SHARP 3-W LEDs exhibit a luminous reduction of about 20%. However, when mounted on a heat sink with $R_{hs} = 1.8$ °C/W, they only have a luminous reduction of 10%. Similar results are obtained from the Luxeon 1-W LEDs, which have less luminous reduction when mounted on a larger heat sink with a smaller R_{hs}.

Several observations can therefore be made from these results, from which some insights into the design guidelines of LED systems can be derived.

1) Some differences between the measured and calculated curves are observed. Such differences might be due to the assumptions made in the theoretical calculations. The assumption that all LED devices are identical and share the same temperature and power is not exactly true in practice. In fact, there are variations among LEDs of the same type and even of the same bin. The efficacy reduction rate k_e is also affected by the ageing of the LED devices. Nevertheless, the dynamic PET theory can predict the general trends of the luminous flux output as functions of time fairly accurately.
2) It is important for the LED system designers and product manufacturers to use the steady-state luminous flux and efficacy as rated values if the LED systems are used continuously. However, for applications in which the LED systems are turned on momentarily, a different time-dependent curve should be selected.
3) The amount of luminous flux reduction depends on the thermal design and is more serious in LED systems using heat sinks with high thermal resistance (as predicted

in both steady-state and dynamic theories). In order to reduce the luminous reduction of an LED system, it is necessary to design a heat sink with good cooling effects.

4) The results in Fig. 16–18 indicate that the luminous flux outputs of the same number of LEDs mounted on different heat sinks are initially close to each other because the temperature rise of the heat sinks is not significant initially. This implies that, for temporary applications such as traffic lights in which the amber light is turned on typically 5 s and the green light is turned on 25 to 120 s, a small heat sink is sufficient. Therefore, the luminous flux, as predicted by this dynamic theory, with a small time can be used as the designed luminous flux.
5) However, for continuous operation such as road lighting, the luminous flux projected at the steady state should be used as the prediction. It is therefore necessary to ensure that the thermal design can meet the luminous requirements at steady-state operation.

V. Conclusion

A dynamic PET theory has been developed and practically verified. The main contribution of this paper is the introduction of the time domain and, thus, dynamics to the steady-state PET theory. This dynamic PET theory confirmed by practical measurements highlights the time dependence of the luminous flux of an LED system. The luminous flux of an LED system tends to decrease with time because of the gradual temperature rise in the heat sink and, therefore, the junction of the LED. This means that LED systems with continuous and discontinuous operation should be designed according to different time-dependent luminous flux curves. This theory opens a door to the accurate prediction of the luminous flux output for a given LED system design. Three types of LEDs have been modeled and practically tested with different heat sinks. The practical and theoretical results obtained for these LED systems are generally in good agreement, confirming the validity of the dynamic PET theory. This dynamic theory enables the study of the photometric, electric, thermal, and temporal aspects of an LED system in a systematic manner and provides a tool for the optimal design of LED systems.

Appendix

In the main text of this paper, the thermal time constant of the LED package is much smaller (typically a thousand times smaller in practice) than that of the heat sink. Equation (7) thus assumes that the heat-sink temperature T_{hs} remains constant during the fast transient. The thermal dynamics of the heat sink is handled separately. If this assumption is removed, a more vigorous analysis is presented here.

In Fig. 1, the heat will flow from the equivalent heat source through the thermal resistor (P_1), and another portion of the heat will flow into the thermal capacitor (P_{Cj}) of the LED package. Based on thermal circuit analysis, it can be shown that

$$P_{C_j} = Nk_hP_d - P_1 \tag{A1}$$

$$P_{C_j} = NC_{jc}\frac{d(T_j - T_a)}{dt} \tag{A2}$$

$$P_1 = \frac{T_j - T_{hs}}{R_{jc}/N}. \tag{A3}$$

Based on (A1)–(A3), we have the relationships

$$NC_{jc}\frac{d(T_j - T_a)}{dt} = Nk_hP_d - \frac{T_j - T_{hs}}{R_{jc}/N} \tag{A4}$$

$$T_{hs} = R_{jc}C_{jc}\frac{dT_j}{dt} + T_j - R_{jc}k_hP_d \tag{A5}$$

$$\frac{dT_{hs}}{dt} = R_{jc}C_{jc}\frac{d^2T_j}{dt^2} + \frac{dT_j}{dt}. \tag{A6}$$

for the heat sink.

The items T_{hs} and dT_{hs}/dt expressed in (A5) and (A6) can be used in (12). Now, putting (A5) and (A6) into (12), the differential equation of T_j can be obtained as

$$R_{jc}C_{jc}R_{hs}C_{hs}\frac{d^2T_j}{dt^2} + (R_{jc}C_{jc} + R_{hs}C_{hs} + NR_{hs}C_{jc})\frac{dT_j}{dt} + T_j = (R_{jc} + NR_{hs})k_hP_d + T_a. \tag{A7}$$

Solving (A7), the expression of T_j can be obtained

$$T_j = A_1e^{\lambda_1 t} + A_2e^{\lambda_2 t} + (R_{jc} + NR_{hs})k_hP_d + T_a. \tag{A8}$$

By bringing (A8) into (A5), the heat-sink temperature can be obtained

$$T_{hs} = R_{jc}C_{jc}\lambda_1A_1e^{\lambda_1 t} + R_{jc}C_{jc}\lambda_2A_2e^{\lambda_2 t} + A_1e^{\lambda_1 t} + A_2e^{\lambda_2 t} + NR_{hs}k_hP_d + T_a. \tag{A9}$$

A_1 and A_2 are coefficients which can be determined using the physical boundary condition.

The boundary condition is that, at $t = 0$, the heat-sink temperature and the LED temperature are equal to the ambient temperature

$$T_{hs}(t = 0) = T_a$$
$$T_j(t = 0) = T_a. \tag{A10}$$

Using (A10) into (A8) and (A9), the constants A_1 and A_2 can be obtained.

Therefore, according to (18), the total luminous flux ϕ_v is

$$\begin{aligned}\phi_v &= NEP_d \\ &= NE_o\left[1 + k_e(T_a - T_o)\right]P_d \\ &\quad + NE_ok_ek_h(R_{jc} + NR_{hs})P_d^2 \\ &\quad + NE_ok_e(A_1e^{\lambda_1 t} + A_2e^{\lambda_2 t})P_d\end{aligned} \tag{A11}$$

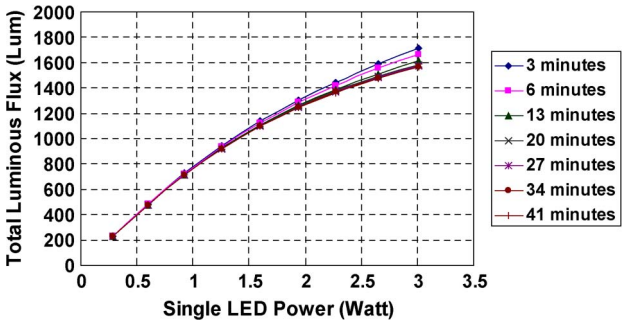

Fig. 19. Calculated luminous flux for eight CREE XLamp XR-E LEDs mounted on a heat sink with $R_{hs} = 1.8$ °C/W by the vigorous analysis.

where

$$\lambda_1 = \frac{\sqrt{(R_{jc}C_{jc}+R_{hs}C_{hs}+NR_{hs}C_{jc})^2-4R_{jc}C_{jc}R_{hs}C_{hs}}}{2R_{jc}C_{jc}R_{hs}C_{hs}} - \frac{R_{jc}C_{jc}+R_{hs}C_{hs}+NR_{hs}C_{jc}}{2R_{jc}C_{jc}R_{hs}C_{hs}}$$

$$\lambda_2 = -\frac{\sqrt{(R_{jc}C_{jc}+R_{hs}C_{hs}+NR_{hs}C_{jc})^2-4R_{jc}C_{jc}R_{hs}C_{hs}}}{2R_{jc}C_{jc}R_{hs}C_{hs}} - \frac{R_{jc}C_{jc}+R_{hs}C_{hs}+NR_{hs}C_{jc}}{2R_{jc}C_{jc}R_{hs}C_{hs}}$$

$$A_1 = \frac{k_h P_d + \lambda_2 C_{jc}(R_{jc}+NR_{hs})k_h P_d}{C_{jc}(\lambda_1-\lambda_2)}$$

$$A_2 = \frac{k_h P_d + \lambda_1 C_{jc}(R_{jc}+NR_{hs})k_h P_d}{C_{jc}(\lambda_2-\lambda_1)}.$$

Based on this vigorous analysis, the theoretical luminous flux curves for the test with eight CREE LEDs mounted on a heat sink with $R_{hs} = 1.8$ °C/W are plotted in Fig. 19. The results from this vigorous analysis are very close to the practical measurements in Fig. 10 and the theoretical results using the simplified analysis in Fig. 11.

ACKNOWLEDGMENT

The authors would like to thank B. Ngan for his assistance in obtaining the luminous measurements. The authors would also like to thank the Centre for Power Electronics, City University of Hong Kong, for its support for the project.

REFERENCES

[1] M. Harris, "Let there be light," *IET Eng. Technol. (E&T) Mag.*, vol. 4, no. 20, pp. 18–21, Nov. 21–Dec. 4, 2009.
[2] J. H. Cheng, C. K. Liu, Y. L. Chao, and R. M. Tain, "Cooling performance of silicon-based thermoelectric device on high power LED," in *Proc. 24th Int. Conf. Thermoelectrics*, Clemson, SC, Jun. 2005, pp. 53–56.
[3] T. Zahner, "Thermal management and thermal resistance of high power LEDs," in *Proc. 13th Int. Workshop THERMINIC*, Budapest, Hungary, Sep. 2007, p. 195.
[4] J. Garcia, D. G. Lamar, M. A. Costa, J. M. Alonso, and M. R. Secades, "An estimator of luminous flux for enhanced control of high brightness LEDs," in *Proc. IEEE Power Electron. Spec. Conf.*, Rhodes, Greece, Jun. 2008, pp. 1852–1856.
[5] C. Biber, "LED light emission as a function of thermal conditions," in *Proc. IEEE Semicond. Therm. Meas. Manage. Symp.*, San Jose, CA, Mar. 2008, pp. 180–184.
[6] L. Trevisanello, M. Meneghini, G. Mura, M. Vanzi, M. Pavesi, G. Meneghesso, and E. Zanoni, "Accelerated life test of high brightness light emitting diodes," *IEEE Trans. Device Mater. Rel.*, vol. 8, no. 2, pp. 304–311, Jun. 2008.
[7] S. Y. R. Hui and Y. X. Qin, "A general photo-electro-thermal theory for light-emitting-diode (LED) systems," *IEEE Trans. Power Electron.*, vol. 24, no. 8, pp. 1967–1976, Aug. 2009.
[8] L. Yuan, S. Liu, M. X. Chen, and X. B. Luo, "Thermal analysis of high power LED array packaging with microchannel cooler," in *Proc. 7th ICEPT*, Shanghai, China, Aug. 2006, pp. 1–5.
[9] J. Petroski, "Spacing of high-brightness LEDs on metal substrate PCB's for proper thermal performance," in *Proc. 9th Intersoc. Conf. Therm. Thermomech. Phenom. Electron. Syst., ITHERM*, Las Vegas, NV, Jun. 2004, pp. 507–514.
[10] M. Arik, C. Becker, S. Weaver, and J. Petroski, "Thermal management of LEDs: Package to system," *Proc. SPIE*, vol. 5187, pp. 64–75, 2004.
[11] Q. Cheng, "Thermal management of high-power white LED package," in *Proc. 8th ICEPT*, Shanghai, China, Aug. 2007, pp. 1–5.
[12] J. Lalith, Y. M. Gu, and N. Nadarajah, "Characterization of thermal resistance coefficient of high-power LEDs," in *Proc. 6th Int. Conf. Solid State Lighting*, San Diego, CA, Aug. 2006, pp. 63 370–63 377.
[13] M. Nishikawa, Y. Ishizuka, H. Matsuo, and K. Shigematsu, "An LED drive circuit with constant-output-current control and constant-luminance control," in *Proc. INTELEC*, Providence, RI, Sep. 2006, pp. 1–6.
[14] K. Hwu and S. Chou, "A simple current-balancing converter for LED lighting," in *Proc. IEEE Appl. Power Electron. Conf.*, Washington, DC, Feb. 2009, pp. 587–590.
[15] Y. Hu and M. M. Jovanovic, "LED driver with self-adaptive drive voltage," *IEEE Trans. Power Electron.*, vol. 23, no. 6, pp. 3116–3125, Nov. 2008.
[16] P. Baureis, "Compact modeling of electrical, thermal and optical LED behavior," in *Proc. 35th Eur. Solid-State Device Res. Conf.*, Grenoble, France, Sep. 2005, pp. 145–148.
[17] Y. X. Qin, D. Y. Lin, and S. Y. R. Hui, "A simple method for comparative study on the thermal performance of light emitting diodes (LED) and fluorescent lamps," *IEEE Trans. Power Electron.*, vol. 24, no. 7, pp. 1811–1818, Jul. 2009.
[18] H. J. Chiu, Y. K. Lo, J. T. Chen, S. J. Cheng, C. Y. Lin, and S. C. Mou, "A high-efficiency dimmable LED driver for low-power lighting applications," *IEEE Trans. Ind. Electron.*, vol. 57, no. 2, pp. 735–743, Feb. 2010.
[19] X. Tao and S. Y. R. Hui, "A general photo-electro-thermo-temporal theory for light-emitting diode (LED) systems," in *Proc. IEEE ECCE*, 2010, pp. 184–191.
[20] S.-C. Tan, "General n-level driving approach for improving electrical-to-optical energy-conversion efficiency of fast-response saturable lighting devices," *IEEE Trans. Ind. Electron.*, vol. 57, no. 4, pp. 1342–1353, Apr. 2010.

Xuehui Tao was born in China. She received the B.S. degree in electronic science and technology and the M.S. degree in electronic engineering from Southwest Jiaotong University, Chendu, China. She is currently working toward the Ph.D. degree in the Centre for Power Electronics, City University of Hong Kong, Kowloon, Hong Kong.

Her current research interests include LED thermal modeling, LED system design, and power electronic system integration.

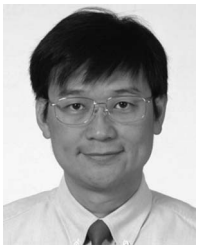

S. Y. Ron Hui (F'03) received the B.Sc.(Hons.) degree in engineering from the University of Birmingham, Birmingham, U.K., in 1984, and the D.I.C. and Ph.D. degrees from the Imperial College of Science and Technology, London, U.K., in 1987.

He has previously held academic positions at the University of Nottingham, Nottingham, U.K., and the University of Sydney, Sydney, Australia. He joined the City University of Hong Kong (CityU), Kowloon, Hong Kong, as a Professor in 1996 and was promoted to Chair Professor in 1998. In 2001–2004, he served as an Associate Dean of the Faculty of Science and Engineering, CityU. From July 2011, he holds the Chair Professorships at both the University of Hong Kong and Imperial College London. He has published over 200 technical papers, including more than 140 refereed journal publications and book chapters. Over 50 of his patents have been adopted by industry.

Dr. Hui is a Fellow of the Institution of Engineering and Technology (IET). He has been an Associate Editor (Power Conversion) of the IEEE TRANSACTIONS ON POWER ELECTRONICS since 1997 and an Associate Editor (Lighting Technology) of the IEEE TRANSACTIONS ON INDUSTRIAL ELECTRONICS since 2007. He has been appointed twice as an IEEE Distinguished Lecturer by the IEEE Power Electronics Society in 2004 and 2006. He served as one of the 18 Administrative Committee members of the IEEE Power Electronics Society and was the Chairman of its Constitution and Bylaws Committee from 2002–2010. He was the recipient of the Excellent Teaching Award at CityU in 1998 and the Earth Champion Award in 2008. He was the recipient of an IEEE Best Paper Award from the IEEE Industry Applications Society Committee on Production and Applications of Light in 2002 and two IEEE TRANSACTIONS ON POWER ELECTRONICS Prize Paper Awards for his publication in wireless battery charging platform technology in 2009 and for his paper on LED system theory in 2010. His inventions on wireless charging platform technology underpin key dimensions of Qi, the world's first wireless power standard, with freedom of positioning and localized charging features for the wireless charging of consumer electronics. In November 2010, he was the recipient of the IEEE Rudolf Chope R&D Award from the IEEE Industrial Electronics Society and of the IET Achievement Medal (The Crompton Medal) and was elected to the Fellowship of the Australian Academy of Technological Sciences and Engineering.